

REPORT DOCUMENTATION PAGE

Form Approved
OMB No. 0704-0188

Public reporting burden for this collection of information is estimated to average 1 hour per response, including the time for reviewing instructions, searching existing data sources, gathering and maintaining the data needed, and completing and reviewing this collection of information. Send comments regarding this burden estimate or any other aspect of this collection of information, including suggestions for reducing this burden to Department of Defense, Washington Headquarters Services, Directorate for Information Operations and Reports (0704-0188), 1215 Jefferson Davis Highway, Suite 1204, Arlington, VA 22202-4302. Respondents should be aware that notwithstanding any other provision of law, no person shall be subject to any penalty for failing to comply with a collection of information if it does not display a currently valid OMB control number. **PLEASE DO NOT RETURN YOUR FORM TO THE ABOVE ADDRESS.**

1. REPORT DATE (DD-MM-YYYY) 10-10-2008		2. REPORT TYPE Technical Paper & Briefing Charts		3. DATES COVERED (From - To)	
4. TITLE AND SUBTITLE Preliminary Study of Heat Transfer Correlation Development and Pressure Loss Behavior in Curved High Aspect Ratio Coolant Channels				5a. CONTRACT NUMBER	
				5b. GRANT NUMBER	
				5c. PROGRAM ELEMENT NUMBER	
6. AUTHOR(S) Jennifer C. Nathman, Justin E. Niehaus, & J. Chris Sturgis (AFRL/RZSE); Anh-Tuan Le & Jung Yi (Advatech Pacific)				5d. PROJECT NUMBER	
				5e. TASK NUMBER	
				5f. WORK UNIT NUMBER 50260312	
7. PERFORMING ORGANIZATION NAME(S) AND ADDRESS(ES) Air Force Research Laboratory (AFMC) AFRL/RZSE 4 Draco Drive Edwards AFB CA 93524-7160				8. PERFORMING ORGANIZATION REPORT NUMBER AFRL-RZ-ED-TP-2008-432	
9. SPONSORING / MONITORING AGENCY NAME(S) AND ADDRESS(ES) Air Force Research Laboratory (AFMC) AFRL/RZS 5 Pollux Drive Edwards AFB CA 93524-7048				10. SPONSOR/MONITOR'S ACRONYM(S)	
				11. SPONSOR/MONITOR'S NUMBER(S) AFRL-RZ-ED-TP-2008-432	
12. DISTRIBUTION / AVAILABILITY STATEMENT Approved for public release; distribution unlimited (PA #08424A).					
13. SUPPLEMENTARY NOTES For presentation at the 55 th JANNAF Propulsion/4 th LPS/3 rd SPS/6 th MSS Joint Meeting, to be held in Orlando, FL, 8-12 Dec 2008					
14. ABSTRACT Convective heat transfer is important for maintaining life and reliability of the main combustion chamber in liquid rocket engines. Enhancing the regenerative cooling circuit's ability to maintain wall temperature with minimal pressure losses improves engine life and has the potential to reduce the turbopump output pressure. High aspect ratio coolant channels have been shown to reduce wall temperature with little pressure increase. Additionally, rocket engine cooling circuits are curved and the mechanisms responsible for curvature enhancement remain unclear for tall, narrow passages and appropriate predictive tools have not been developed. The objective of this research is to study the mechanisms responsible for improved cooling performance and to develop heat transfer correlations for use in high aspect ratio coolant channels having conducting side walls and subjected to asymmetric heating on the concave side, thus modeling a channel in a slotted liner.					
15. SUBJECT TERMS					
16. SECURITY CLASSIFICATION OF:			17. LIMITATION OF ABSTRACT	18. NUMBER OF PAGES	19a. NAME OF RESPONSIBLE PERSON
a. REPORT	b. ABSTRACT	c. THIS PAGE			19b. TELEPHONE NUMBER <i>(include area code)</i>
Unclassified	Unclassified	Unclassified	SAR	43	N/A

**PRELIMINARY STUDY OF HEAT TRANSFER CORRELATION DEVELOPMENT AND
PRESSURE LOSS BEHAVIOR IN CURVED HIGH ASPECT RATIO COOLANT CHANNELS**

Jennifer C. Nathman, Justin E. Niehaus, and J. Chris Sturgis
Liquid Rocket Engines Branch (AFRL/RZSE)
Air Force Research Laboratory
Edwards AFB, CA

Anh-Tuan Le and Jung Yi
Advatech Pacific Incorporated
Redlands, CA

ABSTRACT

Convective heat transfer is important for maintaining life and reliability of the main combustion chamber in liquid rocket engines. Enhancing the regenerative cooling circuit's ability to maintain wall temperature with minimal pressure losses improves engine life and has the potential to reduce the turbopump output pressure. High aspect ratio coolant channels have been shown to reduce wall temperature with little pressure increase. Additionally, rocket engine cooling circuits are curved and the mechanisms responsible for curvature enhancement remain unclear for tall, narrow passages and appropriate predictive tools have not been developed. The objective of this research is to study the mechanisms responsible for improved cooling performance and to develop heat transfer correlations for use in high aspect ratio coolant channels having conducting side walls and subjected to asymmetric heating on the concave side, thus modeling a channel in a slotted liner. Tests are conducted with water in a single, curved channel subjected to heat flux on the outer radius wall and in a straight channel with heat input to an analogous wall. Analyses are done in three areas. First, correlations are developed as functions of Reynolds number, Prandtl number, ratio of viscosities, aspect ratio, axial location, and curvature based on experimental data. Analysis shows that approximately 96% of curved channel data are predicted to within $\pm 10\%$ by the resulting Nusselt number correlations. The average percent difference between the data and predicted value is approximately 3% of the predicted value. This indicates that the correlations properly capture the trends and yield useful predictions of heat transfer. Secondly, published correlations are evaluated at each angular location capture current data trends well. Lastly, analysis examines effect of curvature on pressure gradients. Computational fluid dynamics is incorporated to provide insight into mechanisms responsible for pressure losses. Radial pressure gradients start forming approximately 11 hydraulic diameters upstream of the start of curvature and continue approximately 18 hydraulic diameters downstream of the end of curvature. The data found in this investigation is of good quality and will be useful when moving to subscale testing.

INTRODUCTION

Proper design of the cooling circuit of a liquid rocket engine is critical for maintaining life and reliability of the combustion chamber. The most challenging location for accomplishing this design is the throat region due to the elevated hot-gas-side heat flux, geometrical constraints, and curvature of the coolant channel flow path. Fortunately, the curvature provides some enhancement to the coolant-side convection coefficient over that which would be present in a straight channel (Seban and McLaughlin, 1963; McCormack, Welker, Kelleher, 1969; Sturgis and Mudawar, 1999). However, it is unclear whether the mechanisms responsible for this enhancement exist when the coolant channel assumes a high aspect ratio (i.e. tall and narrow

cross-section). Wadel (1998) showed that the hot-gas wall temperature could be lowered with only small increases in pressure losses when examining high aspect ratio coolant channels (HARCC) using an analytic method which was anchored by hot-fire data. All HARCC designs considered lowered hot-gas wall temperature by at least 8% with as little as 2% increase in pressure loss. Wadel concluded that HARCC has an overall benefit, regardless of coolant channel configuration studied.

Implementation of HARCC is becoming more feasible since machining techniques such as milling are now able to fabricate deep, narrow grooves of varying cross-section on contoured surfaces. Therefore, the issue from a design standpoint is to take advantage of both the curvature enhancement and high aspect ratio geometry of the coolant channels with adequate predictive tools and with proper insight into the physics of the interaction.

Relatively few studies have focused on quantifying the effects of high aspect ratio coolant channels and even fewer on the effects of HARCC on curvature enhancement. Also, the effects of HARCC on curvature enhancement mechanisms are not well understood. Therefore, the combination of lack of data and unclear understanding of HARCC presents a design risk when using HARCC. Available heat transfer correlations were developed for tubular passages however they fail to capture the particular characteristics of high aspect ratio channels in a rocket engine cooling circuit; namely, rectangular passage, one-sided heating, temperature gradient in side wall and flow curvature. It is important that the thermal designer understand how the enhancement is influenced by the channel geometry and be able to predict this for different conditions. Since the engine throat represents the most severe thermal environment in the chamber, the consequences of inadequate design tools could cause significant reductions in life and reliability, if not catastrophic failure.

The current research uses a synergistic experimental and computational approach to study curved and straight, asymmetrically-heated, high aspect ratio coolant channels. The overall effort focuses on three aspects: understanding the internal mechanisms; generating new heat transfer correlations; and validating CFD results in order to improve the predictive tools. Moreover, curved channel data are compared to the baseline straight channel experimental data permitting the quantification of the curvature enhancement factor in HARCC. Curved channel experimental data are incorporated in this paper from only aspect ratios 4 and 10, though other tests are ongoing. This paper focuses on generating heat transfer correlations for curved channel data, comparing present correlations to straight channel correlations, assessing several published curvature terms, and investigating curvature effects on pressure losses.

EXPERIMENTAL METHODS

The High Aspect Ratio Coolant Channel (HARCC) Water Flow Loop at the Air Force Research Laboratory is used for testing single straight and curved channels subjected to asymmetric heating. Open to atmosphere, the recirculation loop permits continuous testing while maintaining constant inlet conditions (temperature, pressure, and flow rate) to the test section.

A typical cross-section of the curved copper test channel is shown on in Figure 1 for aspect ratio $AR = 4$. Straight test channel has identical cross-section. The channels are formed by cutting a slot of width, 0.25 in ($W = 6.35$ mm) into a single piece of 102 copper alloy. A T-insert is placed in the slot to form a rectangular flow channel. The length ($L = 15$ in (381 mm)) along the bottom of the rectangular flow channel is the same for both the curved and straight channels. For example, the arc length along the bottom curved channel wall, $S = R_o\pi = L$ equals the heated length of the straight channel, where $R_o = 4.775$ in (121 mm). For the current test matrix, five such T-inserts are used to create aspect ratios of $AR = 1, 2, 4, 8,$ and 10 which correspond to heights of $H = 0.25, 0.5, 1, 2,$ and 2.5 in (6.35, 12.7, 25.4, 50.8, and 63.5 mm). Each of the side walls is half the channel width and the copper is completely enclosed in insulation. The result is a rectangular flow channel with conducting side walls that models a single channel in a regenerative cooling circuit whose land width is equal to the channel width.

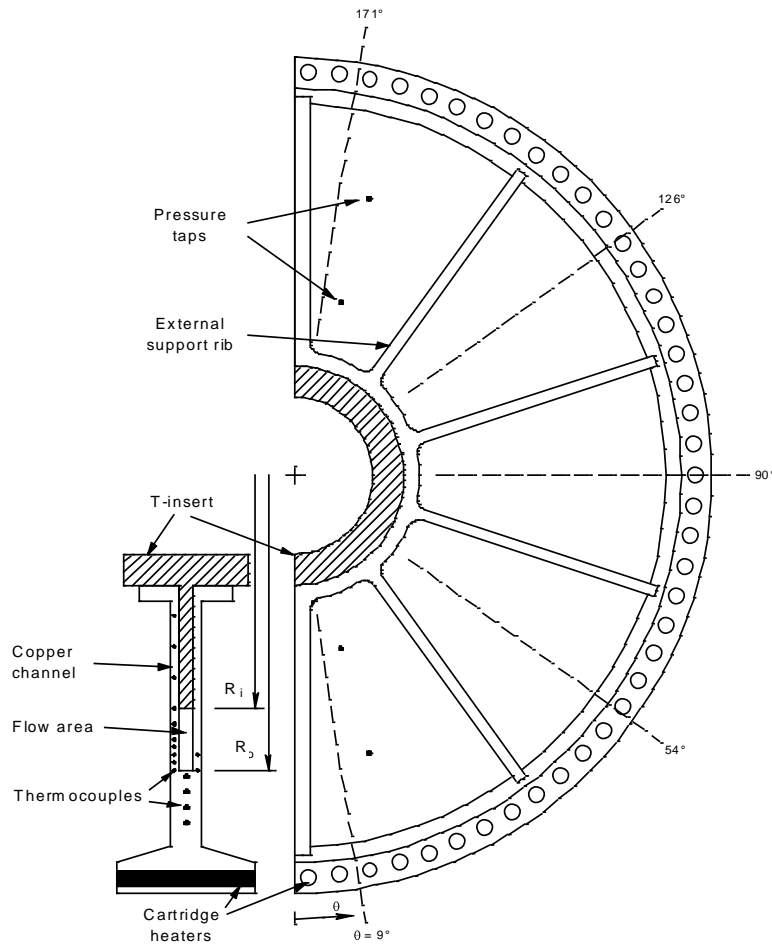


Figure 1. Curved Copper test channel showing thermocouples at five angular locations and the four pressure taps

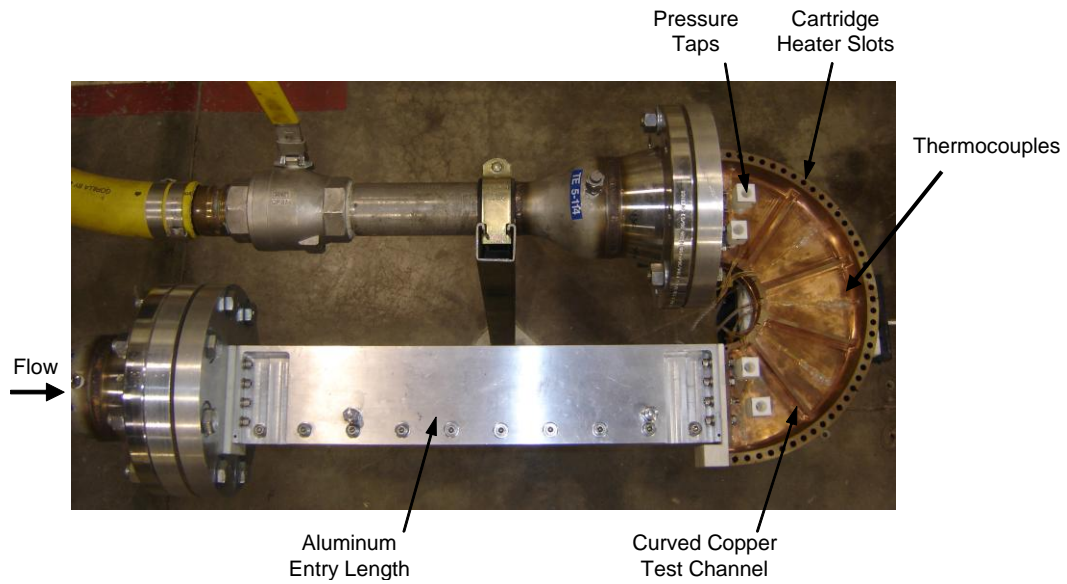


Figure 2. Photo of aluminum entry channel and curved copper test channel connected to water flow loop

The test section consists of two portions: an aluminum entry channel and then a copper test channel which can be straight or curved. For more details about the straight channel see the papers by Sturgis and/or Nathman (2005 and 2007). Figure 2 shows the entry channel with the curved copper channel installed in the flow loop ready for testing with the exception of insulation which has been removed for clarity in illustrating the test rig. The unheated entry channel provides a fully developed turbulent flow into the heated copper test section with a length of 508 mm corresponding to 80 hydraulic diameters (D_h) in length for $AR = 1$ and $44D_h$ for $AR = 10$. In any given test configuration, both channels have the same internal passage geometry.

Heat is applied at the outer radius by 41 cartridge heaters embedded in the base of the copper block (Figs. 1 & 2) connected to a variable voltage source. Due to facility power limitations, heat fluxes up to only 0.8 Btu/in²s (130 W/cm²) could be reached in the curved channel whereas 1.1 Btu/in²s (180 W/cm²) is possible in the straight channel. Future upgrades will mitigate this problem. Heat flow to the channel is modeled as one-dimensional in the constant area cross-section since the copper is well insulated.

Thermocouples embedded in the cross-section, shown in Fig. 1, permit the calculation of heat flux and convection coefficient. Three thermocouples in the thick neck section determine the one-dimensional heat flux acting on the channels. Fin thermocouples indicate heat flow up the side walls and into the fluid and are used in the estimation of an average convection coefficient for the cross-section. The array of thermocouples exists at five angular locations in the channel which are indicated in Fig. 1 and visible in Fig. 2. This permits calculation of heat flux and convection coefficient along the flow. Subsequent discussions will focus on three locations – channel inlet ($\theta = 90^\circ$), mid-channel ($\theta = 90^\circ$), and channel exit ($\theta = 171^\circ$) – which are deemed sufficient to capture the trends. These angular locations correspond to axial locations ($x = 0.75, 7.5,$ and 14.3 in (19.1, 191, and 364 mm)) on the straight channel.

Pressure taps are located near the inlet and exit: $\theta = 15^\circ$ and 165° for the curved channel or $L = 1.25$ and 13.75 in (31.75 and 349.25 mm) for the straight channel. The pressure tap locations allow for measurement of the radial pressure gradient, dP/dr , for $AR = 8$ and 10 . For lower aspect ratios the T-insert interferes with the pressure taps at the top of the channel, so the pressure gradient cannot be measured.

A typical test series begins by configuring the test channel (and entry channel) with a certain aspect ratio and inserting it into the flow loop. After establishing inlet pressure, temperature, and flow rate, the heat input is initiated. Data is recorded at successively higher levels of heat flux, in each case waiting for steady state conditions to prevail. The test concludes at the highest heat fluxes or when the channel wall temperature approaches 212 °F (100 °C).

A new test is initiated by adjusting the flow rate to achieve a different average velocity. Nominally, velocities of $U = 16.4, 32.8, 49.2$ ft/s (5, 10, and 15 m/s) are achieved. These tests are accomplished for two inlet fluid temperatures, $T_{in} = 68$ and 95 °F (20 and 35 °C). This series of tests is repeated for each of the five aspect ratios examined, with several extra tests to assess repeatability. Therefore, the experimental heat transfer data is collected for ranges of axial location ($1.7 \leq x/D_h \leq 57$), heat flux ($0.06 (10) \leq q'' \leq 0.8$ Btu/in²-s (130 W/cm²)), Reynolds number ($50,000 \leq Re_{D_h} \leq 300,000$), fluid temperature ($T_{in} = 68, 95$ °F) and aspect ratio ($AR = 4$ and 10). The inlet pressure is held constant at 30 psi (2.1 bars) for all tests. Measurement uncertainties entail: 0.7 °F for T_b ; 0.125 psi (0.0086 bar) for pressure; 3.5% max for U ; 30% for low q'' (0.092 Btu/in²-s (15 W/cm²)) decreasing to 13% or less for $q'' > 0.24$ Btu/in²-s (40 W/cm²) which represents most data; \bar{h} and Nu will be slightly more than q'' due to calculation assumptions; Re uncertainty is similar to U ; dP/dr uncertainty is similar to pressure.

Several potential parameters governing curved flow have been identified. The first is purely a geometric term – the ratio of diameter of curvature to diameter of flow passage. It is less clearly defined for a rectangular passage since the diameter of curvature (d_c) could be interpreted as twice the distance from the center of curvature to the center of the cross-section or to the heated wall. The difference can be significant with high aspect ratio coolant channels. The diameter of

the flow passage is usually taken as the hydraulic diameter. The second is the Dean number which is defined as

$$De = Re \sqrt{\frac{D_h}{d_c}} \quad (1)$$

and represents the ratio of the square root of the product of inertial and centrifugal (pressure) forces to the viscous forces (Berger et al., 1983). A third term is the centripetal acceleration experienced by the fluid non-dimensionalized by earth's gravitational constant, g_e . This also is subject to selection of the curvature dimension, but for the present work will be defined as

$$g^* = \frac{U^2}{R_o g_e} \quad (2)$$

where R_o is the radius at the channel outer wall. The ranges of these parameters are: $21 \leq 2R_o/D_h \leq 24$; $6,000 \leq De \leq 66,000$; and $21 \leq g^* \leq 190$.

It should be noted that the present test conditions do not represent normal operating environments for rocket engine coolant channels. For example, representative Reynolds number and heat flux values for rocket engine cooling circuits exceeds 1×10^6 and $50 \text{ Btu/in}^2\text{-s}$ ($\sim 8000 \text{ W/cm}^2$), respectively. However, the objective is to understand trends and perform tests at a more feasible level. Computational efforts will be used to extend the insights and correlations developed through these tests to more realistic rocket conditions. Additionally, another research program is under way to examine HARCC by means of a small combustion chamber which can achieve higher Reynolds numbers and heat fluxes. These tests will complement the present investigation and validate the computational results. The test section is instrumented such that validation and appropriate analysis can be done.

Data reduction proceeds from measured temperatures, flow rates, pressures, and key assumptions. Average velocities are calculated from measured flow rate and channel cross-sectional area. Fluid inlet temperature is measured by a thermocouple inserted into the flow. Bulk temperature (T_b) at each of the axial instrumentation locations is calculated based on known flow rate, fluxes up to the point of interest, and the assumption of a well-mixed flow. Water properties such as density, viscosity, thermal conductivity, and Prandtl number are considered functions of only bulk temperature. Applied heat flux (q'') derived from the copper temperature gradient in the neck region (indicated by thermocouples) and assumption of constant copper conductivity ($0.0052 \text{ Btu/in-s-R}$ (390 W/m-K)).

The convection coefficient is derived from an energy balance, measured temperatures and certain assumptions. The applied heat load (in neck region) is equated to the heat transferred to the fluid by convection plus that conducted up the fin beyond the flow passage. Estimations indicate that losses through the side insulation are negligible. Convection to the fluid is estimated by integration along the channel surface using measured fin (wall) temperatures and assumption of a bulk fluid temperature. Conduction up the fin beyond the flow passage is estimated by the temperature gradient in the fin at the top of the flow passage and is negligible. The energy balance yields an average convection coefficient, \bar{h} , for the cross-section where it is understood that \bar{h} pertains to only three walls. A convection coefficient is determined for each flux value recorded at three axial locations – near the inlet, midway along the channel, and near the exit. Corresponding Nusselt numbers are calculated by multiplying the convection coefficient by hydraulic diameter and dividing by the water conductivity. For detailed descriptions of the experimental setup and data reduction refer to papers by Sturgis and Nathman (2007 and 2005).

RESULTS AND DISCUSSION

This initial examination of $AR = 4$ and 10 experimental heat transfer data is used to develop Nusselt number correlations for curved flow, compare curved channel results to straight channel results, and evaluate published curvature terms. Secondly, pressure gradient trends in curved flow are analyzed.

CORRELATION ANALYSIS

The objective of developing Nusselt number correlations is to create a design and analysis tool for the thermal engineer. A correlation's usefulness depends on its ability to accurately predict the heat transfer coefficient for the conditions being examined. These conditions include channel geometry, heating arrangement, fluid characteristics and axial location.

In general, the Nusselt number is correlated with Reynolds and Prandtl numbers following the basic form proposed by Dittus and Boelter (1930). In this expression,

$$Nu = C Re^m Pr^n \quad (3)$$

the unknowns C , m , and n are determined from a least squares fit of the experimental data. The current work takes the initial form and builds on it to eventually create the expanded expression,

$$Nu = C Re^m Pr^n \left(\frac{\mu_b}{\mu_w} \right)^p AR^q \left(1 + \frac{B}{x/D} \right)^r \phi_{cur}^u \quad (4)$$

where unknowns C , m , n , p , q , r , and s are determined from a least-squares best-fit to the experimental data. Equation 4 includes Reynolds number (Re), Prandtl number (Pr), ratio of water viscosity evaluated at bulk temperature and channel base wall temperature (μ_b/μ_w), aspect ratio (AR), thermal flow development ($1+B/(x/D)$), and the curvature parameter (ϕ_{cur}). Less critical is the value of B which is chosen in order to avoid large values of the bracketed term at the channel inlet based on the present x/D_h data. In this paper only results from $AR = 4$ and 10 will be presented. Since correlations will be developed for each aspect ratio, the AR term is omitted from this best-fit analysis due to its singular value. Due to delays in analysis, the value of exponent u and the curvature parameter will only be examined using values found in literature.

Two figures of merit are used to assess the quality of the correlation in representing the data. First, the average percent difference (a.p.d.) is defined as the difference between the experimental and predicted values as a percentage of the predicted correlation value. These are averaged over the number of data points. Secondly, the number of data points (on a percent basis) that fall within $\pm 10\%$ of the predicted values indicates the degree to which the correlation captures the data trend.

The analysis begins with the general form of the Nusselt correlations. It applies the least-squares best-fit method to curved experimental data at the inlet location ($\theta = 90^\circ$) for $AR = 4$ across all velocities, heat fluxes, and inlet temperatures while employing the hydraulic diameter and bulk temperature. The resulting correlation,

$$Nu = 0.118 Re^{.68} Pr^{.26} \quad (5)$$

captures 96% of the data within $\pm 10\%$ of the predicted values with an average percent difference (a.p.d.) of 3.3. This correlation was generated over 84 steady state data points. Similar results are achieved when the analysis is performed for the mid-channel ($\theta = 90^\circ$) and exit ($\theta = 171^\circ$) locations, with 98 % and 100 % of data points falling within $\pm 10\%$ of the respective correlations.

This indicates that at any one angular location the data trend is very consistent and describable with each expression generated.

With the addition of the viscosity ratio term to the general form of the equation, no increase occurs in the percentage of data captured for the inlet and mid-channel locations when using the same set of experimental data as before. However, a 2% decrease is found for the exit location. Regardless of the decrease, all the correlations generated thus far are of good quality.

A similar process is applied to $AR = 10$ curved channel experimental data under the same conditions. Resulting correlations from the general form at the inlet, mid-channel, and exit locations captures 95% or greater of the data within $\pm 10\%$ of the predicted values, respectively. Corresponding a.p.d. values are 3.6 or lower. Figure 3 is an example of the correlation generated in the general form using mid-channel data. These correlations are each generated over 78 steady state data points. Expressions with the appended viscosity term result in approximately the same percentages and average percent differences.

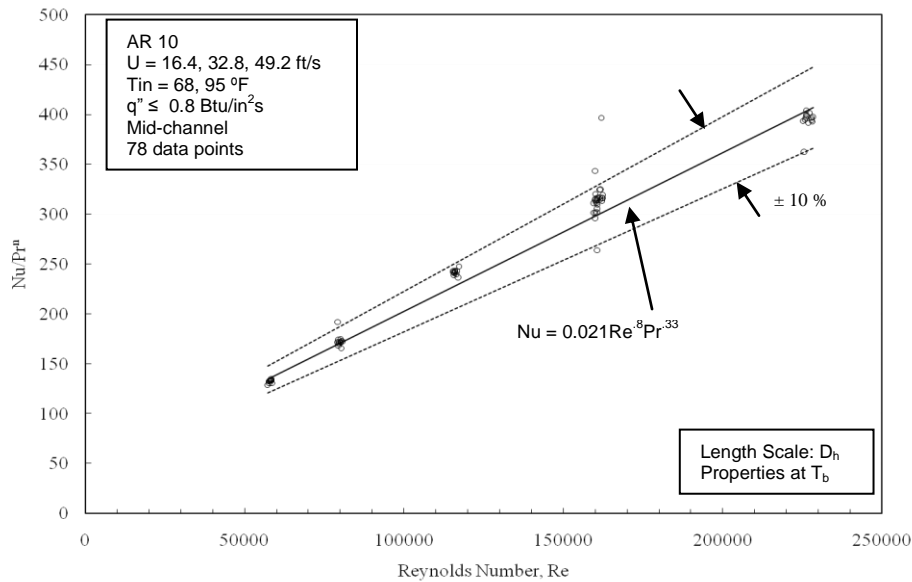


Figure 3. Nusselt Number Correlation of Present Data

The next step is to create correlations applicable for a broader range of data and assess their quality. This data set encompasses all angular locations ($\theta = 9^\circ, 90^\circ,$ and 171°), heat fluxes, and inlet temperatures for $AR = 4$ curved channel tests. Hydraulic diameter and bulk temperature are used and the data set contains 252 data points. Both expressions shown here,

$$Nu = 0.071 Re^{.71} Pr^{.31} \tag{6}$$

$$Nu = 0.071 Re^{.71} Pr^{.31} \left(\frac{\mu_b}{\mu_w} \right)^{.0172} \tag{7}$$

where the percent captured decreases by 50% and the a.p.d. doubles for both expressions. The decrease in the percent captured is attributed to entrance effects such as thermal boundary layer development. The correlations created from an analogous set of 234 data points for $AR = 10$ only decrease about 10%. For aspect ratio 10, the thermal boundary layer may be smaller thus a smaller reduction in the percent captured compared to aspect ratio 4. Since the percentages for both aspect ratios decrease this implies that a term is needed to address thermal development.

Reconsidering all angular locations for $AR = 4$ and determining the best-fit correlation for this yields

$$Nu = 0.066Re^{.71}Pr^{-.3} \left(\frac{\mu_b}{\mu_w} \right)^{.03} \left(1 + \frac{10}{x/D_h} \right)^{.0703} \quad (8)$$

where the average percent difference is 10.5 and 52% of the data is captured within $\pm 10\%$. The addition of the axial location term does not improve correlation quality for aspect ratio 4 over the results from Equations 6 and 7. This indicates another term is needed in the correlation to improve quality or use only data from the downstream locations that is more thermally developed. This paper will address the later of the two options now and the first option later with the addition of published curvature terms. As for $AR = 10$, the resulting correlation with its corresponding data set provides an a.p.d. of 5.2 and captures 92% of the data within $\pm 10\%$. The high percentage for aspect ratio 10 shows that the development of the thermal boundary layer has less of an impact on correlation quality when compared to aspect ratio 4.

In order to further increase correlation quality, data from the inlet location are omitted to reduce entrance effects. This results in a percent captured of 99% with an a.p.d. equal to 1.9 for $AR = 4$ and 96% and 3.4 for $AR = 10$. The corresponding correlations for aspect ratios 4 (168 data points) and 10 (148 data points) are shown below in Equations 9 and 10. These are more accurate predictors of Nusselt number, although with the added restriction that $x/D_h \geq 15$. Also, notice the exponents for the viscosity ratio and axial location terms have different signs. The exponents for these terms tend to be negative for all expressions for aspect ratio 10 regardless of the data sets used.

$$Nu = 0.014Re^8Pr^{-.36} \left(\frac{\mu_b}{\mu_w} \right)^{.1} \left(1 + \frac{10}{x/D_h} \right)^{1.42} \quad AR = 4 \quad (9)$$

$$Nu = 0.020Re^{.82}Pr^{-.37} \left(\frac{\mu_b}{\mu_w} \right)^{-.01} \left(1 + \frac{10}{x/D_h} \right)^{-.454} \quad AR = 10 \quad (10)$$

Heat transfer data collected from straight channel testing have been put through the same correlation analysis as described above for the curved channel heat transfer data. Correlations follow similar trends in the curved channel correlations, except the addition of the viscosity ratio term to the general form (Eq. 3) increases the percent captured considerably. Detailed straight channel analyses can be found in Nathman and Sturgis (2008) and Sturgis (2008), which include other comparisons such as varying the length scale and the temperature for which to evaluate the fluid properties. Their results show that employing the width as the length scale resulted in slightly better correlations with the hydraulic diameter, but not significantly enough to dissuade use of the well-accepted hydraulic diameter. Also, no difference in the correlation quality occurred when evaluating fluid properties with the film temperature as opposed to bulk temperature. These comparisons are not included in this preliminary curved channel analysis. This analysis continues to apply the hydraulic diameter and the bulk temperature; however, future analyses may revisit these comparisons.

The second aspect of the correlation analysis involves examining the effect of curvature terms on correlation quality. The curvature terms of interest found in literature are summarized in Table 1 and will be inserted into Equation 11. Also Eq. 11 will be applied to each angular location and downstream locations (i.e. mid-channel and exit locations). Sturgis and Mudawar (1999) and Sturgis and Nathman (2008) provide lists of curvature terms. When affixing Ito's curvature term to the expression and setting the value of exponent u to 1, such that

$$Nu = C Re^m Pr^n \left(\frac{\mu_b}{\mu_w} \right)^p \varphi_{cur}^u \quad (11)$$

the resulting correlations capture above 94% of the data for each angular location regardless of aspect ratio. However, applying Eq. 11 to just the downstream locations, the percentage drops to 14% for aspect ratio 4. For $AR = 10$ the percentage stayed the same (~ 94%). Modifications to Eq. 11 such as adding the thermal flow development parameter when using larger data sets do not yield better results.

Several authors found Ito's curvature term suitable for their heat transfer correlations for curved flow. Seban and McLaughlin (1963) use the Dittus and Boelter equation with the film temperature and Ito's enhancement term. Performance is low evaluating Eq. 11 using the appropriate properties. Also, applying their entire expression captures below 5% of the present data. Rogers and Mayhew (1964) used the same equation as Seban and McLaughlin, but instead used the bulk temperature which captured less than 15% of the present data. Though both of these studies used water, the configuration was such that the tube was heated around the entire periphery. Taylor's (1968) equation was only applied to the current data sets for each aspect ratio using downstream locations because it includes an axial location term. The percentage of data captured was below 6% because the slope of the data and the correlation are different. Taylor's equation tends to over predict the Nusselt values.

Table 1. Published Curvature Terms		
Author	Curvature term, φ_{cur}	Comments
Ito (1959)	$\varphi_{cur} = Re^{.05} \left(\frac{D}{d_c} \right)^{.1}$	Limited to $Re(D/dc)^2 > 6$
Sturgis and Mudawar (1999)	$\varphi_{cur} = Re_D^{.046} \left(\frac{D_h}{2R_o} \right)^{.1}$	Developed for the exit location and $AR = 2$
Niino et al. (1982)	$\varphi_{cur} = Re_D^{.02} \left(\frac{D_h}{d_c} \right)^{.04} \left[1 + \sin \left(\pi \sqrt{\frac{x_c}{L_c + 15D_h}} \right) \right]$	Developed for rectangular, asymmetrically heated passages
Pratt (1947)	$\varphi_{cur} = 1 + 3.4 \left(\frac{D}{d_c} \right)$	Developed for full-periphery heated coiled tubes

Sturgis and Mudawar's (1999) curvature term is inserted into Equation 11. High percentages of data (~ 94%) fall within 10% of the resulting expression when applying it to each angular location and aspect ratio. Percentages drop to 40% for $AR = 4$ when examining data for downstream locations. Sturgis and Mudawar developed this curvature term to apply to the exit location, so the inclusion of data at the mid-channel and exit locations is outside the applicability of the term. The percentages for $AR = 10$ remain high; approximately 94% for the mid-channel and exit locations combined.

Secondly, the correlations developed by Sturgis and Mudawar for each angular location are applied to the current data set at each corresponding location. None of the correlations captured any data because they over predict the current data. This was an unusual finding because

Sturgis and Mudawar conducted similar testing for aspect ratio 2, but with a different working fluid. For example, the correlation Sturgis and Mudawar developed for the exit location is given in Eq. 12. As an exercise, the values for the coefficient and Reynolds number and Prandtl number exponents are calculated from the best-fit method while the curvature term exponent is fixed at unity for AR = 4. Equation 13 is the resulting expression using the exit channel data with bulk temperature and hydraulic diameter. Notice the coefficient and Reynolds number exponent decrease causing the percent captured to increase to 100% between Eq. 12 and 13. (These equations differ from Eq. 11 because the viscosity ratio term is omitted.)

$$Nu = 0.0302Re^{.808}Pr^{.4} \left(Re^{.046} \left(\frac{D_h}{2R_o} \right)^{.1} \right) \tag{12}$$

$$Nu = 0.0272Re^{.749}Pr^{.403} \left(Re^{.046} \left(\frac{D_h}{2R_o} \right)^{.1} \right) \tag{13}$$

Next, the curvature term from Niino et al. (1982) is evaluated in a similar manner. Inserting their enhancement term into Eq. 11 captures over 94% of the data when considering each angular location. The results differ from Sturgis and Mudawar where 98% of the data is captured for the mid-channel and exit locations for aspect ratio 4 as opposed to aspect ratio 10 where only 5% of the data is captured. Lastly, the full equation developed by Niino et al. does not capture any of the current data regardless of how the data is sorted.

Results similar to those previously described are obtained when employing Pratt’s (1947) curvature enhancement term. Equation 11 with Pratt’s curvature term produces the same results as Ito’s term applied to data sets of each angular location and downstream locations from different locations for each aspect ratio.

Another way to evaluate the curvature terms from Table 1 is graphically. These curvature terms are plotted in Figure 4 along with curved-to-straight channel Nusselt number data for AR = 4 at the exit location.

Notice the slopes are approximately the same between the data and the curvature terms. However, the published curvature terms over predict the data. Pratt’s term does not depend on Reynolds number producing in a horizontal line. More analysis should be done by adding more data from other channel locations in order to examine trends over a wider range

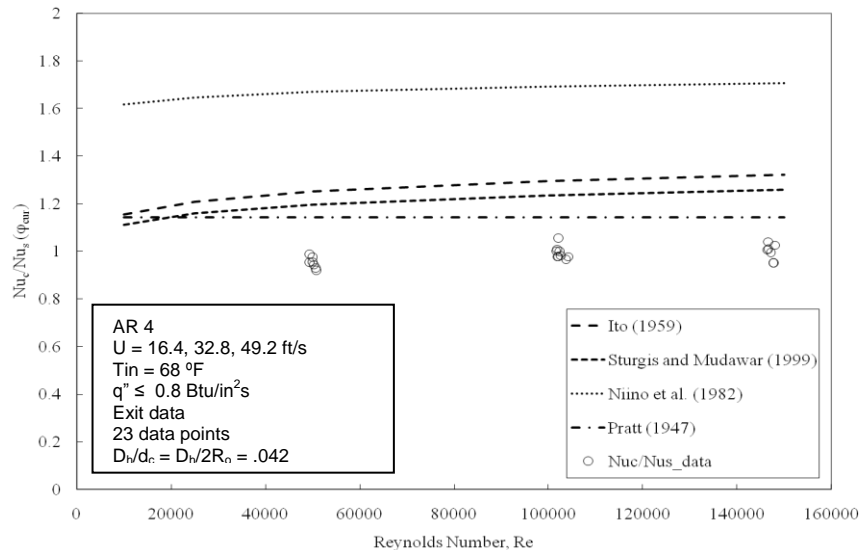


Figure 4. Published Curvature Terms

of data.

PRESSURE GRADIENT

Curvature effects on pressure gradient are examined experimentally. Tests with no heat input were performed for $AR = 4$ and 10 in both curved and straight channels where inlet pressure was held constant at 2.1 bars (30 psia). Two pressure taps located near the inlet and two located near the exit (see Figs. 1 & 2) measured the local radial pressure gradients. The straight channel has four taps in corresponding locations to the curved channel.

Forcing a flow to bend or turn induces secondary flows which mean fluid velocity towards the concave wall increases and fluid velocity near the convex wall decreases (Kakac 1987). For HARCC, the concave wall corresponds to the bottom of the flow area and the convex wall is the top of the channel. Curvature results in radial pressure gradients where high pressure is located near the bottom of the channel and low pressure near the top. The near-inlet and near-outlet radial pressure gradients are plotted in Figure 5 as a function of mean velocity. Notice the radial pressure gradient strength increases as flow moves through the curved channel for aspect ratio 10 . This indicates that the secondary flows are becoming more developed and stronger which would produce a larger pressure gradient at the exit.

The strength of the pressure gradient also relates to centripetal acceleration. Figure 5 shows radial pressure gradients increase with mean velocity. This trend can also be found from a reduction of the Navier-Stokes equations for fully developed flow in a circular curved channel. With no mean radial component of velocity, the Navier-Stokes equation for the radial direction in cylindrical coordinates becomes,

$$\frac{\rho v_{\theta}^2}{r} = \frac{dP}{dr} \quad (14)$$

where ρ is the fluid density, v_{θ} is the tangential velocity. A finite radial pressure gradient exists to balance the centripetal acceleration of the fluid which behaves like U^2/R_0 . The positive dP/dr indicates that pressure increases away from the center of curvature. Equation 14 is shown in Fig. 5 using the current conditions for $AR = 10$ and substitutes $v_{\theta} = U$ and $r = R_0$. It predicts the pressure gradients near the exit of the curved channel over the velocity range tested.

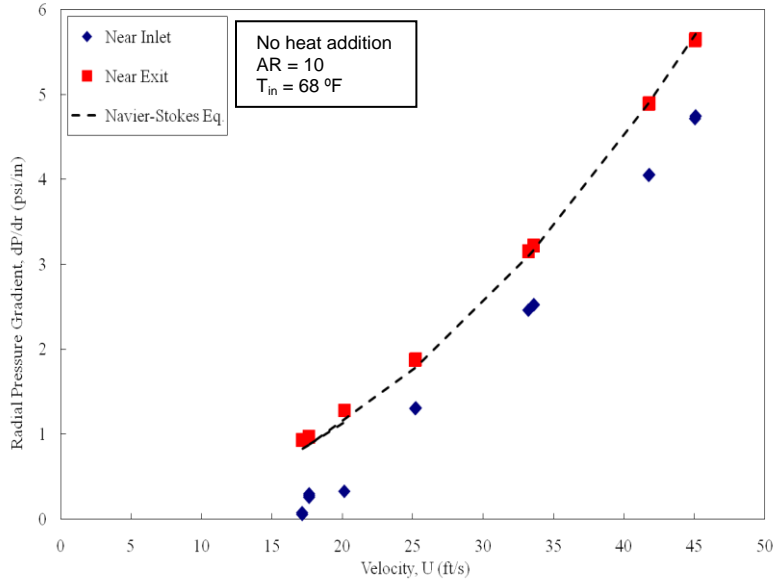


Figure 5. Radial Pressure Gradients with Mean Velocity

Another aspect of curvature effects entails examining the pressure gradients in the flow just upstream of the inlet and immediately downstream of the exit. Since the flow is incompressible, it accounts for flow curvature downstream by forming a radial pressure gradient before the start of curvature. This can be seen in Figure 6, which is a CFD-generated pressure distribution for aspect ratio 10 at a velocity of 49.2 m/s with an adiabatic boundary condition and is the equivalent to an unheated test. Flow is from left to right in the lower branch and the curved section begins at $x = 0$. The CFD results determine that the radial pressure gradient begins forming approximately 11 hydraulic diameters upstream of the inlet and persists until approximately 18 hydraulic diameters downstream of the curved channel exit for the $AR = 10$, $U = 49.2$ ft/s, and $T_{in} = 68$ °F case.

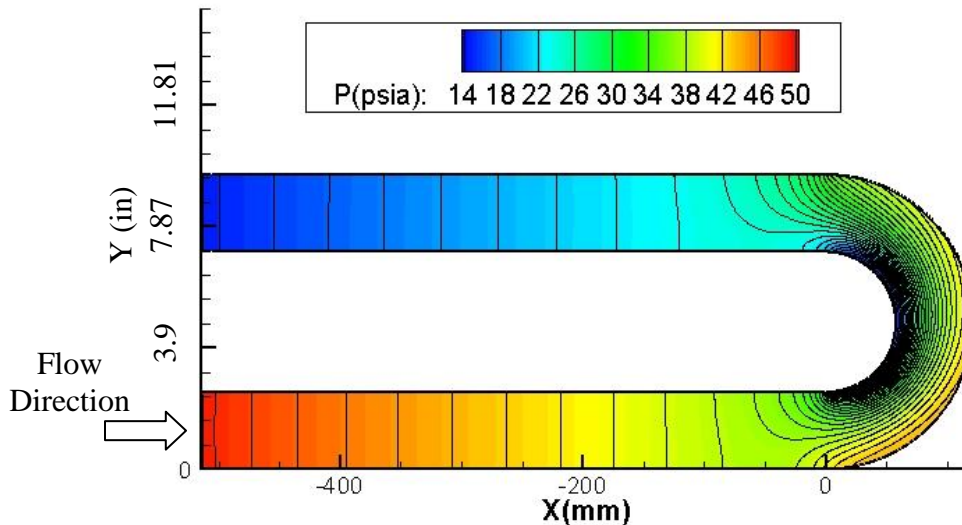


Figure 6. Pressure distribution for $U = 49.2$ ft/s, $T_{in} = 68$ °F with an adiabatic boundary condition.

SUMMARY AND CONCLUSIONS

High aspect ratio curved and straight channel testing is conducted in a test rig which models a channel in a milled-liner chamber. Nusselt number correlations are generated from current $AR = 4$ and 10 curved channel data as functions of Reynolds number, Prandtl number, viscosity ratio, axial location, and curvature. Correlations at each angular location capture the data trend well. Aspect ratio 4 heat transfer correlation that includes all angular locations predicts only 52% of the data within 10% , where as correlation for aspect ratio 10 captures 92% . Low percentages indicate thermal boundary layer development. Improvement in correlation quality is found by omitting inlet data.

Several published curvature terms are appended to the correlations generated with curved channel data. With the addition of most curvature terms, the correlations predicted over 90% of the data at each angular location. However, when an entire published correlation was applied to the data, the data trends were not well captured.

Curvature effects on pressure gradients are examined. The strength of radial pressure gradients directly relates to the centripetal acceleration. A reduced form of the Navier-Stokes equations predicted the near exit radial pressure gradient well. CFD pressure distributions showed the effects of curvature upstream and downstream of the curved channel. Radial pressure gradients begin forming approximately 11 hydraulic diameters upstream of the inlet and persist until approximately 18 hydraulic diameters downstream of the curved channel exit.

FUTURE WORK

Future work entails completing this series of testing ($AR = 1, 2,$ and 8) and modifying the channel to incorporate more instrumentation. CFD work is currently underway to investigate the formation of secondary flows in HARCC. Also, a program is in place that will test at rocket like conditions.

REFERENCES

1. Seban, R.A. and McLaughlin, E.F., ***Heat Transfer in Coiled Tubes with Laminar and Turbulent Flow***, International Journal of Heat and Mass Transfer, Vol. 6, pp. 387-395, 1963.
2. McCormack, P.D., Welker, H. and Kelleher, M., ***Taylor-Goertler Vortices and Their Effect on Heat Transfer***, ASME-AIChE Heat Transfer Conference, Paper 69-HT-3, Minneapolis, MN, 1969.
3. Sturgis, J.C. and Mudawar, I., ***Single-Phase Heat Transfer Enhancement in a Curved, Rectangular Channel Subjected to Concave Heating***, International Journal of Heat and Mass Transfer, Vol. 42, pp. 1255-1272, 1999.
4. Wadel, M.F., ***Comparison of High Aspect Ratio Cooling Channel Designs for Rocket Combustion Chamber with Development of an Optimized Design***, NASA-TM-1998-206313, 1998.
5. Sturgis, J.C., ***Internal Forced Convection in a Straight, Asymmetrically-Heated, High Aspect Ratio Coolant Channel***, 53rd JANNAF Propulsion Meeting, 2nd Liquid Propulsion Subcommittee Meeting, Monterey, CA, December 2005.
6. Nathman, J.C. and Sturgis, J.C., ***Development of Correlations for Use in High Aspect Ratio Coolant Channels***, 54th JANNAF Propulsion Meeting, 3rd Liquid Propulsion Subcommittee Meeting, Denver, CO, May 2007.
7. Sturgis, J. C., and Nathman, J. C., ***Effect of High Aspect Ratio Coolant Channels on Curvature Enhancement***, 54th JANNAF Propulsion Meeting, 3rd Liquid Propulsion Subcommittee Meeting, Denver, CO, May 2007.
8. Berger, S.A, Talbot, L. and Yao, L.S., ***Flow in Curved Pipes***, Annual Review of Fluid Mechanics, Vol. 15, pp. 461-512, 1983.

9. Dittus, F. and Boelter, L., *Heat Transfer in Automobile Radiators of the Tubular Type*, Univ. of California Publications in Engineering, Vol. 2, pp. 443-461, 1930.
10. Ito, H., 1959, *Friction Factors for Turbulent Flow in Pipes*, *ASME Journal of Basic Engineering*, Vol. 81, pp. 123-134.
11. Rogers, G.F.C. and Mayhew, Y.R., 1964, *Heat Transfer and Pressure Loss in Helically Coiled Tubes with Turbulent Flow*, *International Journal of Heat and Mass Transfer*, Vol. 7, pp. 1207-1216.
12. Taylor, M.F., *Heat Transfer Predictions in the Cooling Passages of Nuclear Rocket Nozzles*, Paper 68-608, 4th AIAA Propulsion Joint Specialist Conference, Cleveland, OH, 1968.
13. Niino, M., Kumakawa, A., Yatsuyanagi, N. and Suzuki, A., *Heat Transfer Characteristics of Liquid Hydrogen as a Coolant for the LO₂/LH₂ Rocket Thrust Chamber with the Channel Wall Construction*, Paper AIAA 82-1107, 18th AIAA/SAE/ASME Joint Propulsion Conference, Cleveland, OH, 1982.
14. Pratt, N.H., *The Heat Transfer in a Reaction Tank Cooled by Means of a Coil*, *Transactions of the Institution of Chemical Engineers*, Vol. 25, pp.163-180, 1947.
15. Kakac, S., Shah, R., Aung, W., *Handbook of Single-Phase Convection Heat Transfer*, John Wiley and Sons, NY, 1987.

PRELIMINARY HEAT TRANSFER CORRELATION DEVELOPMENT AND PRESSURE LOSS BEHAVIOR STUDY IN CURVED HIGH ASPECT RATIO COOLANT CHANNELS



**Jennifer C. Nathman, Justin Niehaus,
J. Chris Sturgis,**
Air Force Research Laboratory
Edwards AFB, CA

Anh-Tuan Le, Jung Yi
Advatech Pacific, Inc.
Redlands, CA

JANNAF 6th Modeling and Simulation / 4th Liquid Propulsion /
3rd Spacecraft Propulsion Joint Subcommittee Meeting

December 9, 2008 Orlando, Florida



Outline



- Purpose
- Strategy
- Model/Experimental Set up
- Heat Transfer Correlation Analysis
 - Variation of parameters
 - Comparison to published correlations
- Curvature Effects
 - Pressure loss
- Summary



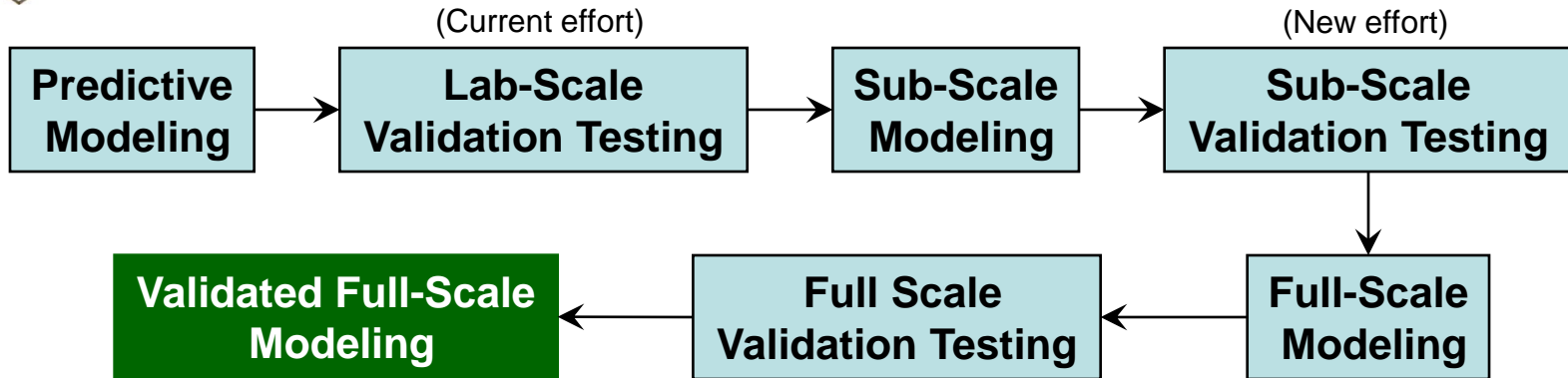
Purpose



- Develop design tools for use with high aspect ratio coolant channels (HARCC)
- Contribute to the thermal management knowledge base of regeneratively cooled liquid rocket engines by
 - Developing correlations
 - Identifying trends
 - Analyzing the fin effects of the channel walls
 - CFD for visualization, understanding, and insight into flow
- Create database with straight and curved channel data



Strategy



- Phase I – Water Flow Loop Testing
 - Straight and curved channels
 - Rich experimental database (AR , Re , q'' , T_{in} , curvature)
 - Develop correlations, predictive tools
 - CFD for insight into flow
 - Limitations: low Re and q'' for rocket applications
- Phase II – Hot-Fire Testing
 - Sub-scale combustion chamber with groups of different sized coolant channels
 - Achieve rocket-like q'' and Re , multiple coolants, validate tools

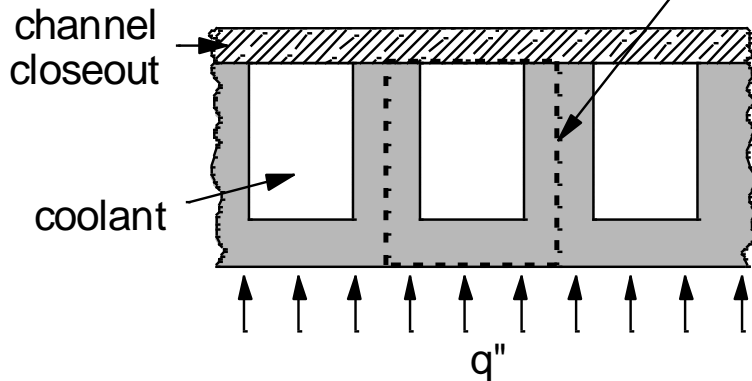
Current effort



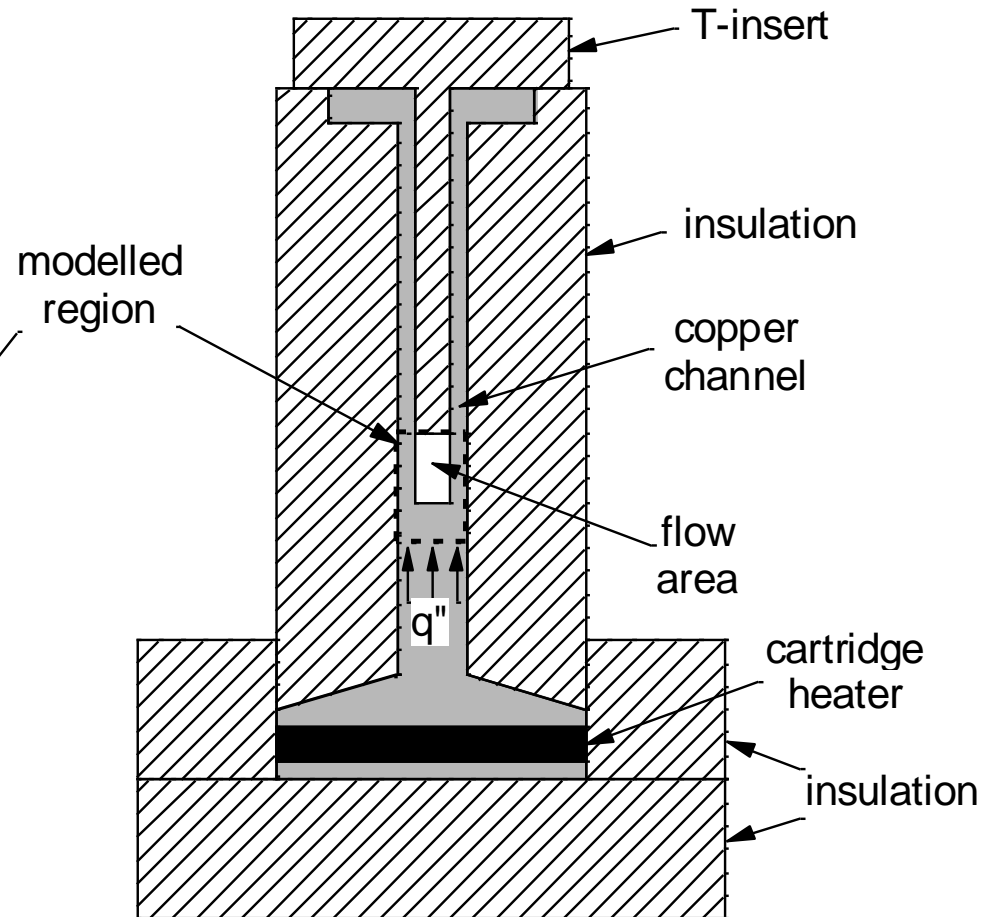
Coolant Channel Model



- Test channel models a rectangular, one-side-heated regen channel with conducting side walls



Milled-liner combustion chamber cross-section



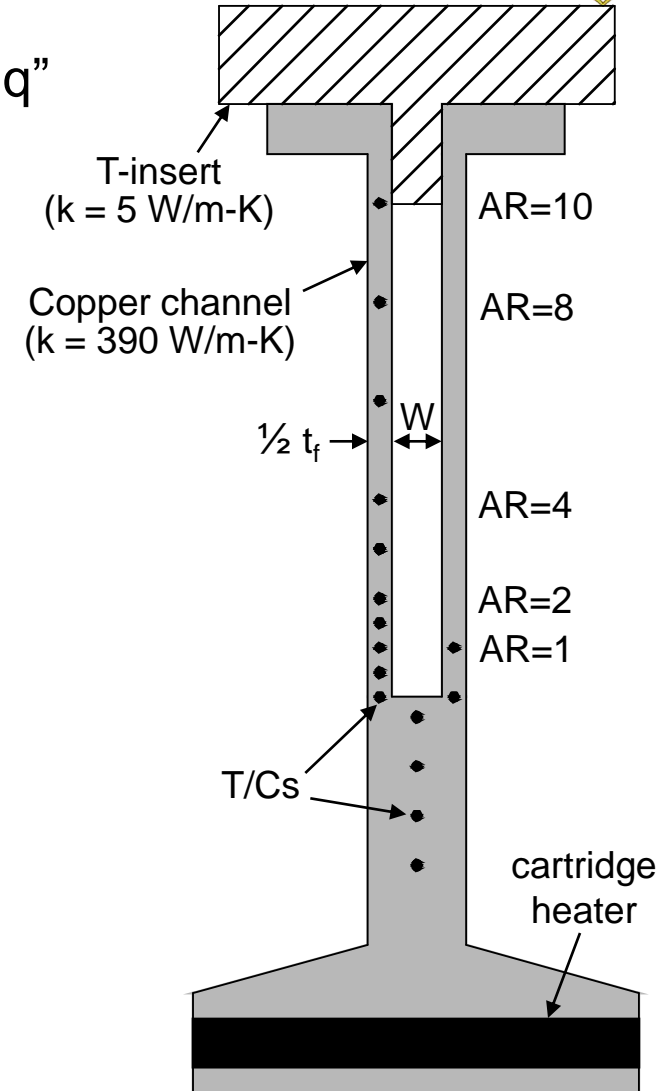
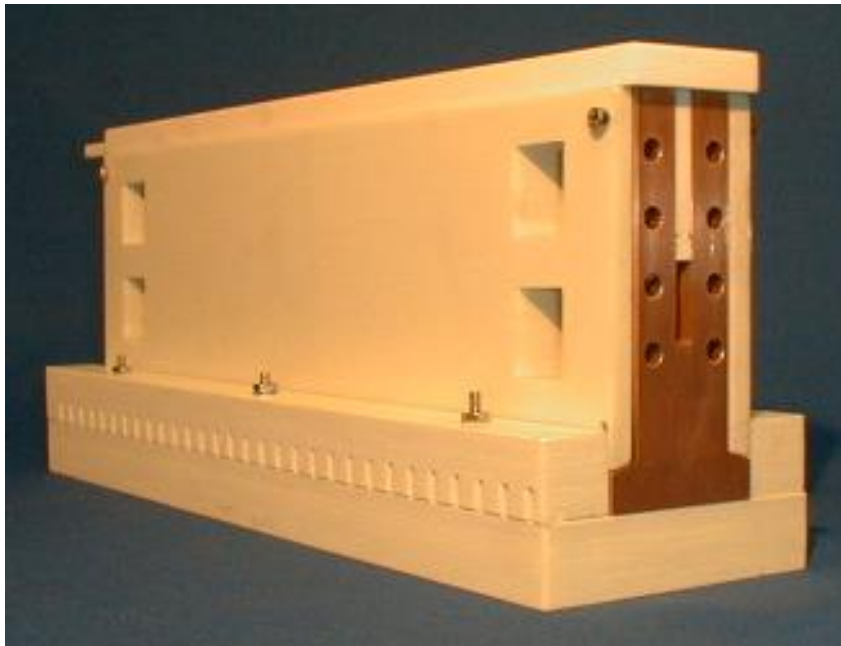
Test channel cross-section



Test Channel Design



- T/Cs in neck measure temp gradient, hence q''
- T/Cs embedded in side walls (fins)
- Heat input adjusted by voltage to heaters
- Channel width to land width, $W:t_f = 1:1$
- One-sided heating, conductive side walls



DISTRIBUTION A, Approved for public release.



Instrumentation

- Length = $\pi R_o = 15$ in
- $U = 5, 10, 15$ m/s
- $Re \leq 300,000$ ($Re_W \leq 180,000$)
- $T_{in} = 20$ or 35 C
- $4.3 \leq Pr \leq 7$
- $AR = 4$ and 10

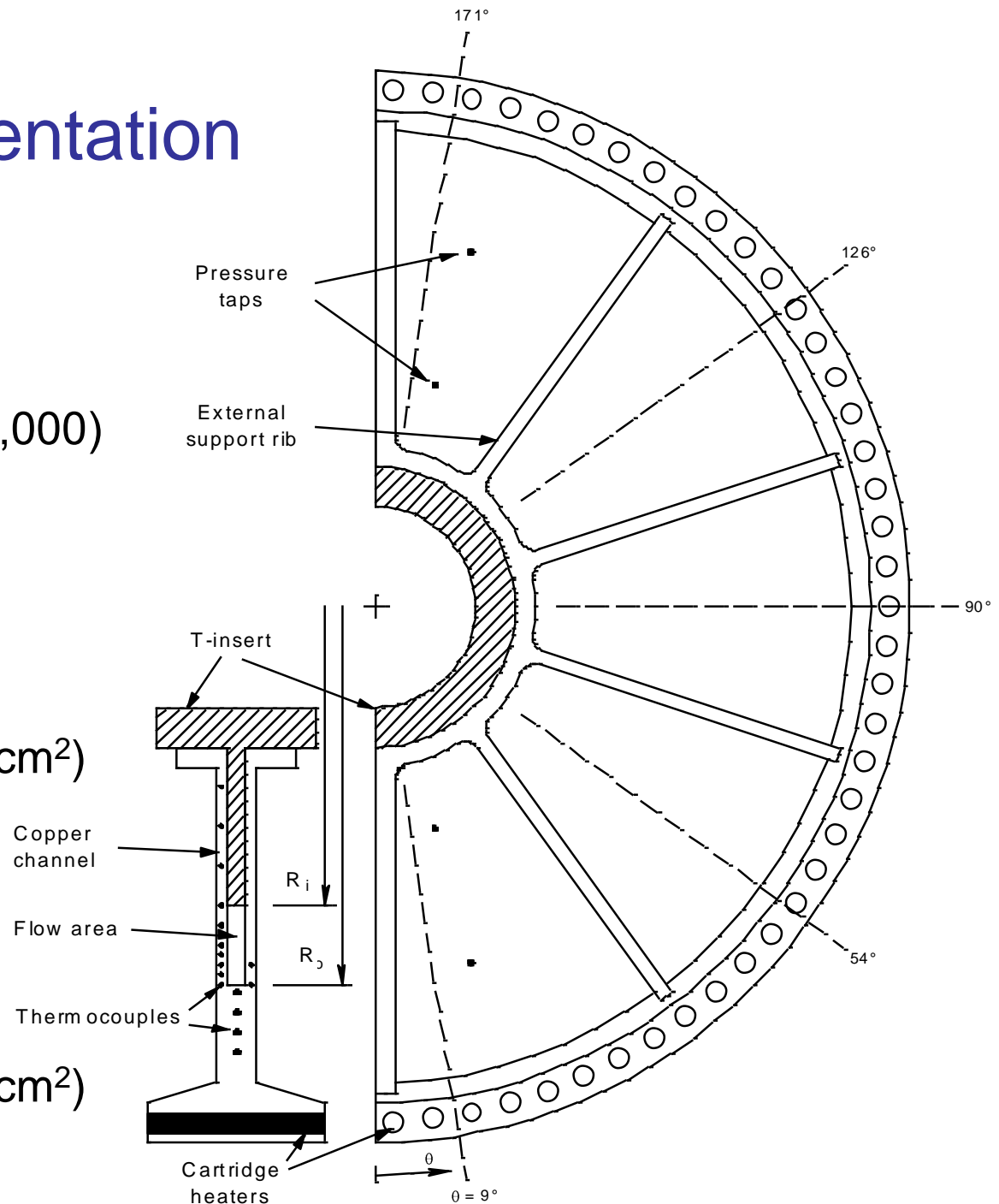
Curved Channel

- $q'' \leq 0.8$ Btu/in²-s (130 W/cm²)
- $21 \leq 2Ro/Dh \leq 24$
- $6,000 \leq De \leq 66,000$
- $21 \leq g^* \leq 190$

Straight Channel

- $q'' \leq 1.1$ Btu/in²-s (180 W/cm²)

DISTR1



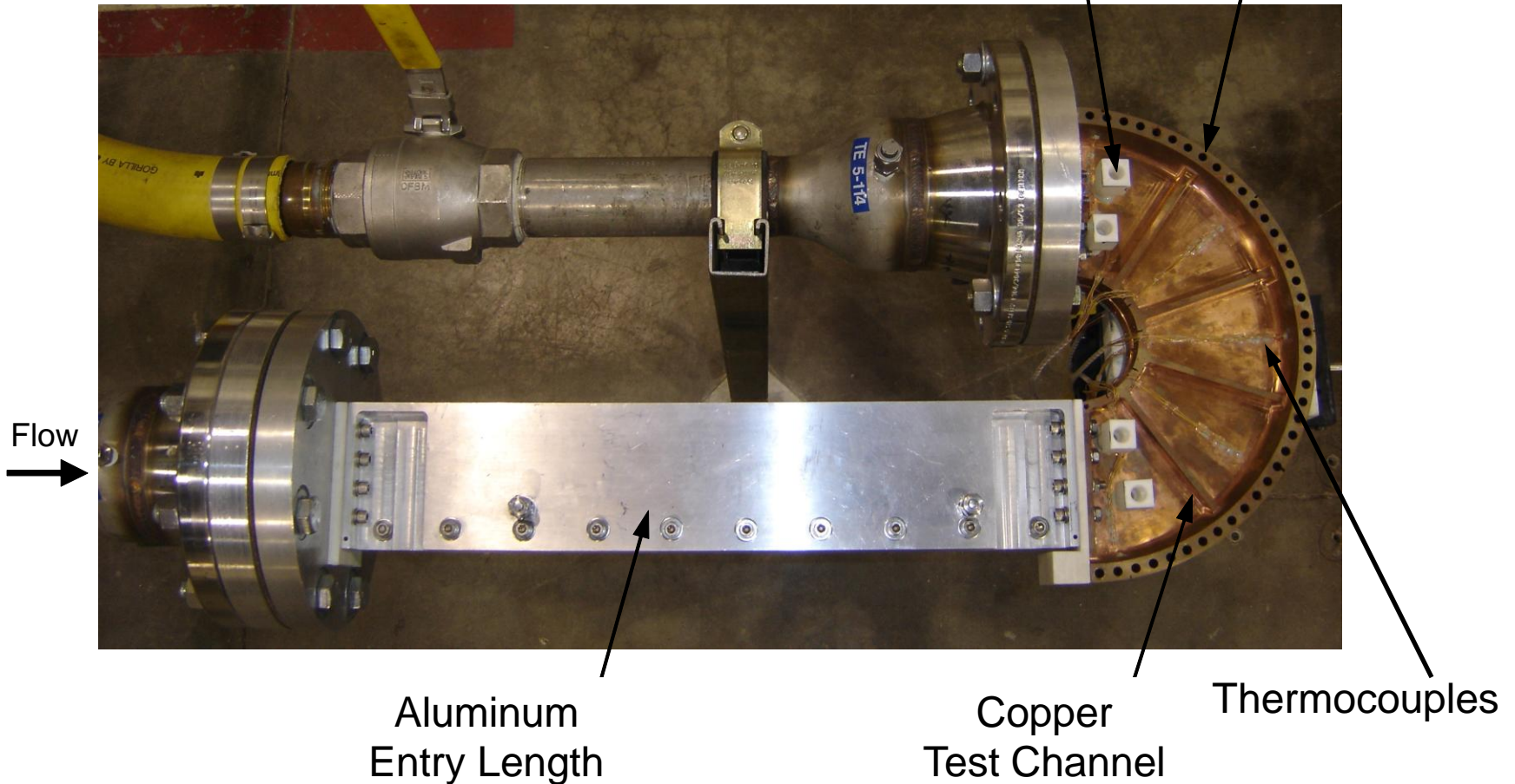


Curved Test Channel in Flow Loop



Pressure
Taps

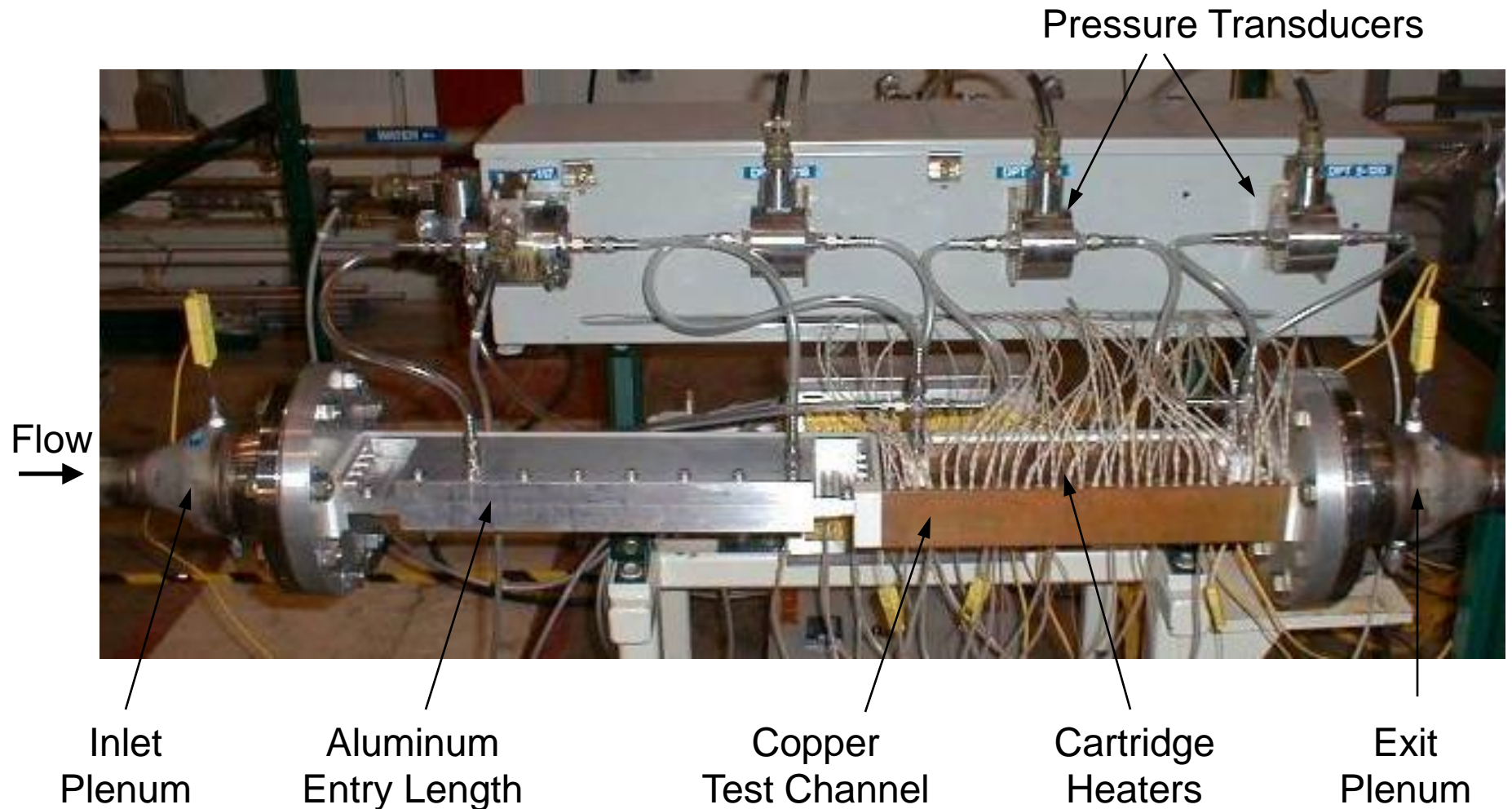
Cartridge
Heater Slots



DISTRIBUTION A, Approved for public release.



Straight Test Channel in Flow Loop



DISTRIBUTION A, Approved for public release.



Data Reduction

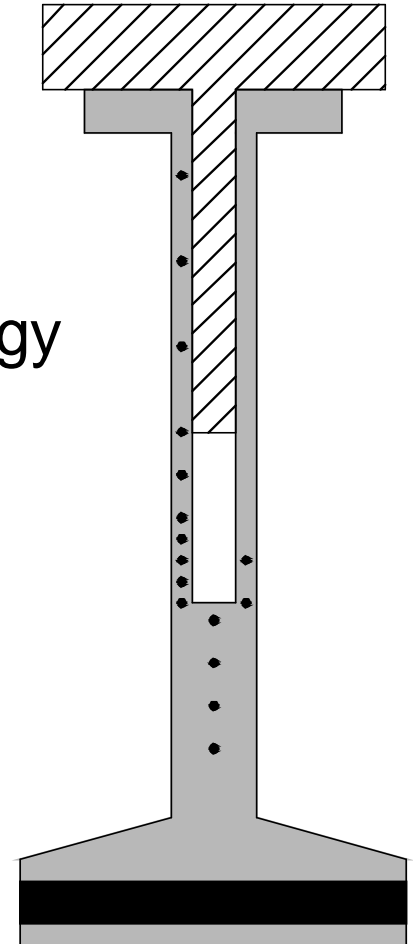


- Local average convection coefficient, \bar{h} , determined over 3 walls at each axial location along channel
- Convection coefficient calculated using an energy balance

Heat input = Heat convected to coolant + Heat loss

- Used in calculating Nusselt numbers (Nu):

$$Nu \equiv \frac{\bar{h}D_h}{k}$$





Correlation Analysis

- Goal: Generate a design and analysis tool that accurately predicts the heat transfer coefficient in a coolant channel (i.e. a Nusselt Number Correlation)

$$Nu = C Re^m Pr^n \left(\frac{\mu_b}{\mu_w} \right)^p AR^q \left(1 + \frac{B}{x/D} \right)^r \phi_{cur}^u$$

- Correlate Nu using a least-squares best fit



Correlation Deduction



- Data sets include:
 - Each aspect ratio (4 or 10)
 - All heat fluxes, velocities, and inlet temperatures
 - 3 axial locations (inlet, mid-channel, exit, and combinations of the 3)
- Parametric Analysis of Nusselt correlations:
 - Addition of terms (example: viscosity ratio)
- Assess the quality of the correlations
 - Average percent difference (a.p.d.)
 - Percentage of data points that fall within +/- 10% of the predicted values (% captured)



Correlation Deduction (cont.): $AR = 4$



- Conditions:
 - Curved channel data, hydraulic diameter, bulk temperature, all inlet temps, $AR = 4$
- Each individual angular location
 - Correlations capture data well (~ 96-100% captured) (84 data points)
- All angular locations (Inlet, mid-channel, and exit)
 - Correlations capture ~ 50 % (252 data points)
 - Thermal Boundary Layer Development - omit inlet data
- Only downstream locations (mid-channel and exit locations, $x/D_h \geq 15$) (168 data points)
(a.p.d / % Captured)

$$Nu = 0.025Re^{.79} Pr^{.38} \quad (12.8 / 19)$$

$$Nu = 0.024Re^{.79} Pr^{.37} \left(\frac{\mu_b}{\mu_w} \right)^{.0526} \quad (12.9 / 14)$$

$$Nu = 0.014Re^{.8} Pr^{.36} \left(\frac{\mu_b}{\mu_w} \right)^{.1} \left(1 + \frac{10}{x/D_h} \right)^{1.42} \quad (1.9 / 99)$$



Correlation Deduction (cont.): $AR = 10$

- Conditions:
 - Curved channel data ,hydraulic diameter, bulk temperature, all inlet temps, $AR = 10$
- Each individual axial location
 - Correlations capture data well (~ 96 % captured) (78 data points)
- All axial locations (Inlet, mid-channel, and exit)
 - Correlations capture ~ 89% (234 data points)
 - Thermal Boundary Layer Development - omit inlet data
- Only downstream locations (mid-channel and exit locations, $x/D_h \geq 15$) (148 data points)
(a.p.d / % Captured)

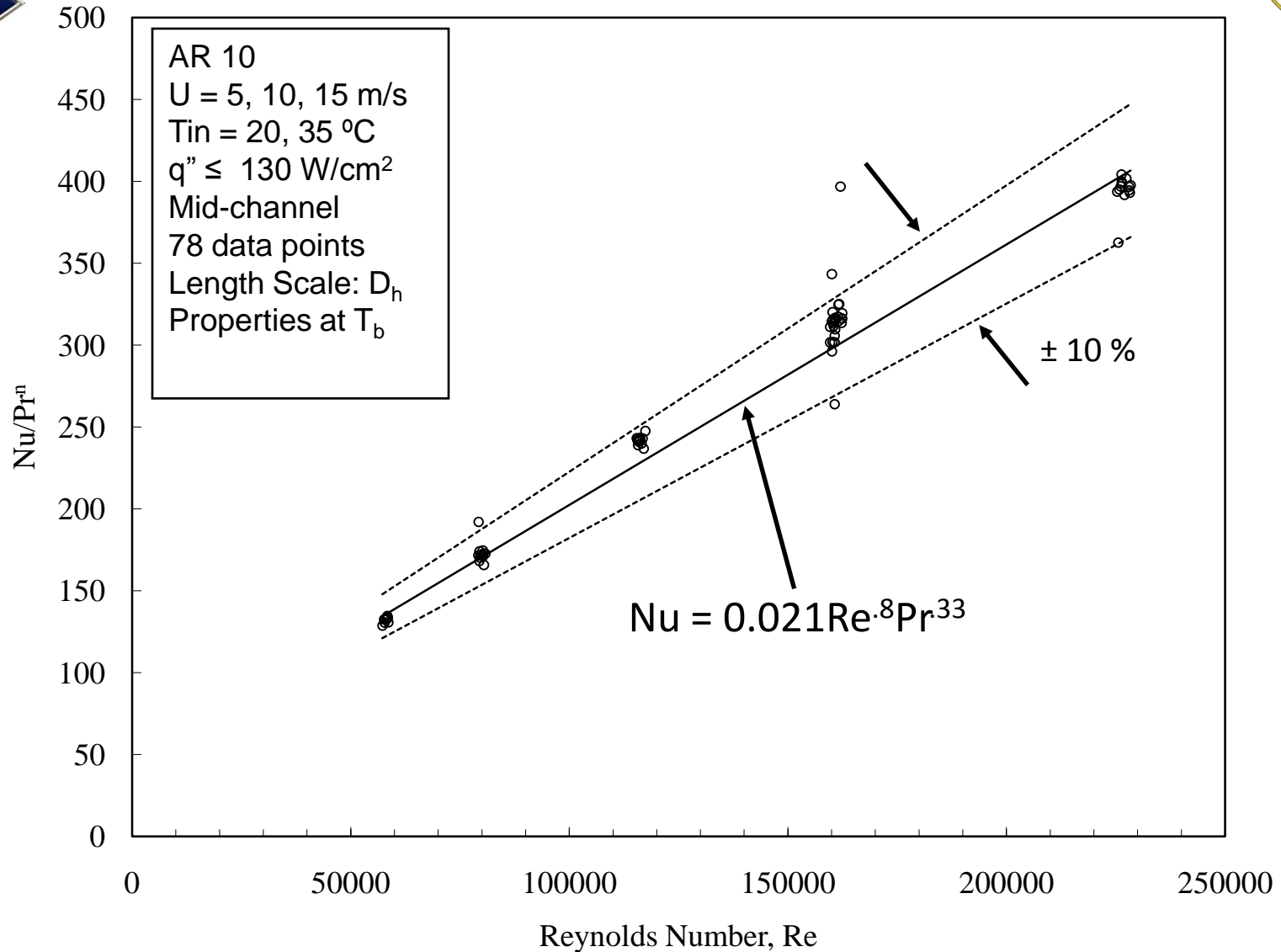
$$Nu = 0.016 Re^{.82} Pr^{.37} \quad (5.1 / 95)$$

$$Nu = 0.018 Re^{.82} Pr^{.37} \left(\frac{\mu_b}{\mu_w} \right)^{-.0312} \quad (5.0 / 94)$$

$$Nu = 0.02 Re^{.82} Pr^{.37} \left(\frac{\mu_b}{\mu_w} \right)^{-.01} \left(1 + \frac{10}{x / D_h} \right)^{-.454} \quad (3.4 / 96)$$



Correlation Deduction (cont.): $AR = 10$



DISTRIBUTION A, Approved for public release.



Straight vs. Curved

- Conditions: hydraulic diameter, bulk temperature, all inlet temps, $AR = 4$
- Only downstream locations (mid-channel and exit locations, $x/D_h \geq 15$)

		(a.p.d / % Captured)
Curved (168 data points)	$Nu = 0.025 Re^{.79} Pr^{.38}$	(12.8 / 19)
	$Nu = 0.024 Re^{.79} Pr^{.37} \left(\frac{\mu_b}{\mu_w} \right)^{.0526}$	(12.9 / 14)
	$Nu = 0.014 Re^{.8} Pr^{.36} \left(\frac{\mu_b}{\mu_w} \right)^{.1} \left(1 + \frac{10}{x/D_h} \right)^{1.42}$	(1.9 / 99)
Straight (430 data points)	$Nu = 0.054 Re^{.73} Pr^{.32}$	(6.9 / 81)
	$Nu = 0.036 Re^{.76} Pr^{.31} \left(\frac{\mu_b}{\mu_w} \right)^{.205}$	(6.6 / 93)
	$Nu = 0.029 Re^{.75} Pr^{.31} \left(\frac{\mu_b}{\mu_w} \right)^{.2} \left(1 + \frac{10}{x/D_h} \right)^{.707}$	(2.1 / 98)



Parametric Results



- Addition of terms
 - Axial location term increases correlation quality
- Curved vs. Straight
 - Different slopes
 - Viscosity ratio increases correlation quality more for straight channel data
- Correlation Limits



Addition of Curvature Terms



- Appending published curvature terms did well at each location
- Low performance for all locations

$$Nu = C Re^m Pr^n \left(\frac{\mu_b}{\mu_w} \right)^p \varphi_{cur}^u$$

Author	Curvature term φ_{cur}	Comments
Ito (1959)	$\varphi_{cur} = Re^{.05} \left(\frac{D}{d_c} \right)^{.1}$	Limited to $Re(D/d_c) > 6$
Sturgis and Mudawar (1999)	$\varphi_{cur} = Re_D^{.046} \left(\frac{D_h}{2R_o} \right)^{.1}$	Developed for the exit location and $AR = 2$
Niino et al. (1982)	$\varphi_{cur} = Re_D^{.02} \left(\frac{D_h}{d_c} \right)^{.04} \left[1 + \sin \left(\pi \sqrt{\frac{x_c}{L_c + 15D_h}} \right) \right]$	Developed for rectangular, asymmetrically heated passages
Pratt (1947)	$\varphi_{cur} = 1 + 3.4 \left(\frac{D}{d_c} \right)$	Developed for full-periphery heated coiled tubes



Curvature Terms (cont.)



- Addition of curvature terms at each angular location capture data trends well for AR 4 and 10 (~94%)
- Percentages low when evaluated using all angular locations
- Ito's term:
 - 14% for mid-channel and exit angular locations for AR 4
 - 94% for mid and exit angular locations for AR 10
- Using Pratt term had same results as Ito

$$Nu = C Re^m Pr^n \left(\frac{\mu_b}{\mu_w} \right)^p \Phi_{cur}^u$$



Curvature Terms (cont.)

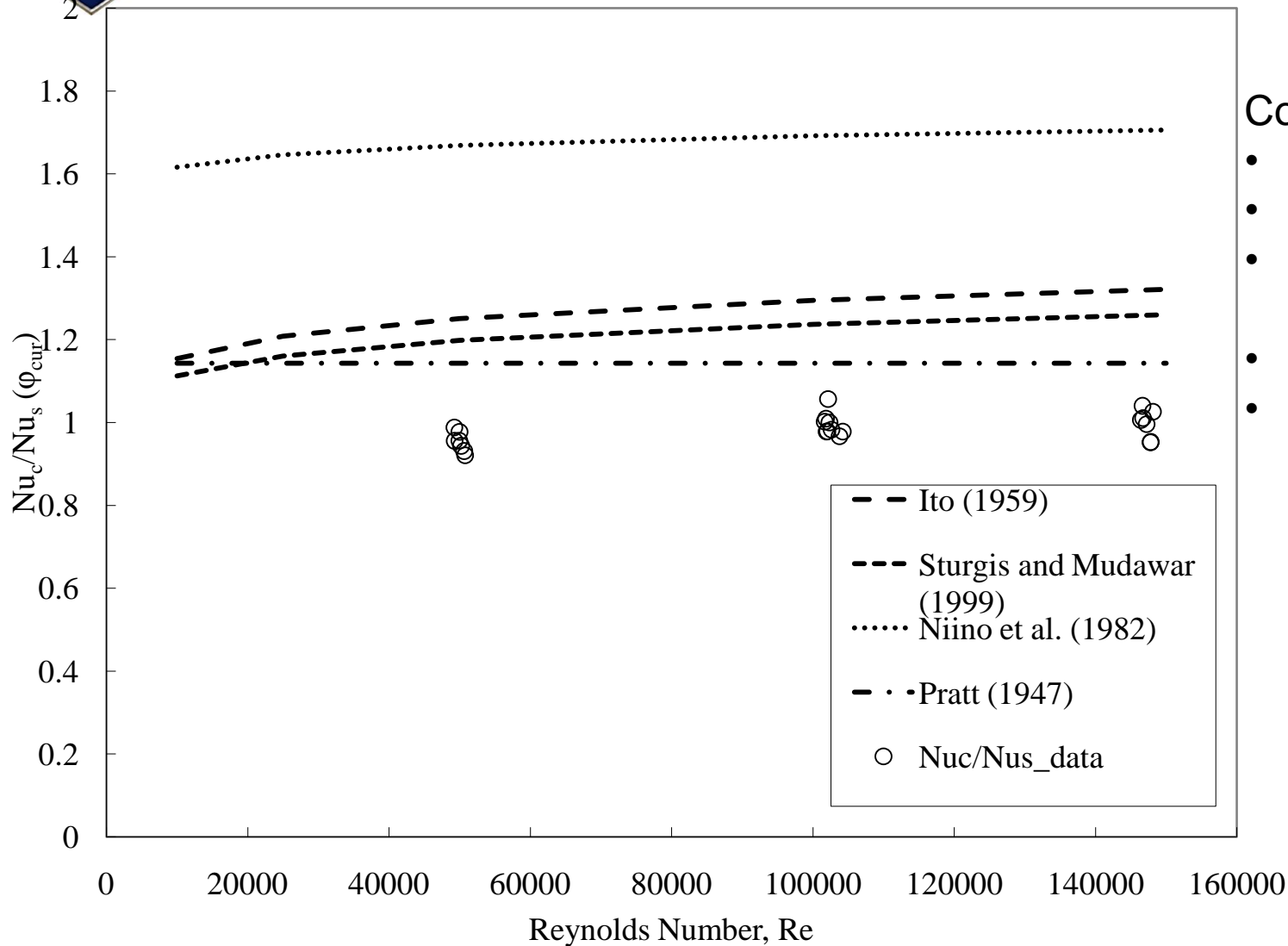


- Sturgis and Mudawar
 - 40% for downstream angular locations for AR 4
 - 94% for downstream angular locations for AR 10
- Niino
 - 98% for mid and exit angular locations for AR 4
 - 5% for mid and exit angular locations for AR 10

$$Nu = C Re^m Pr^n \left(\frac{\mu_b}{\mu_w} \right)^p \varphi_{cur}^u$$



Published Curvature Terms



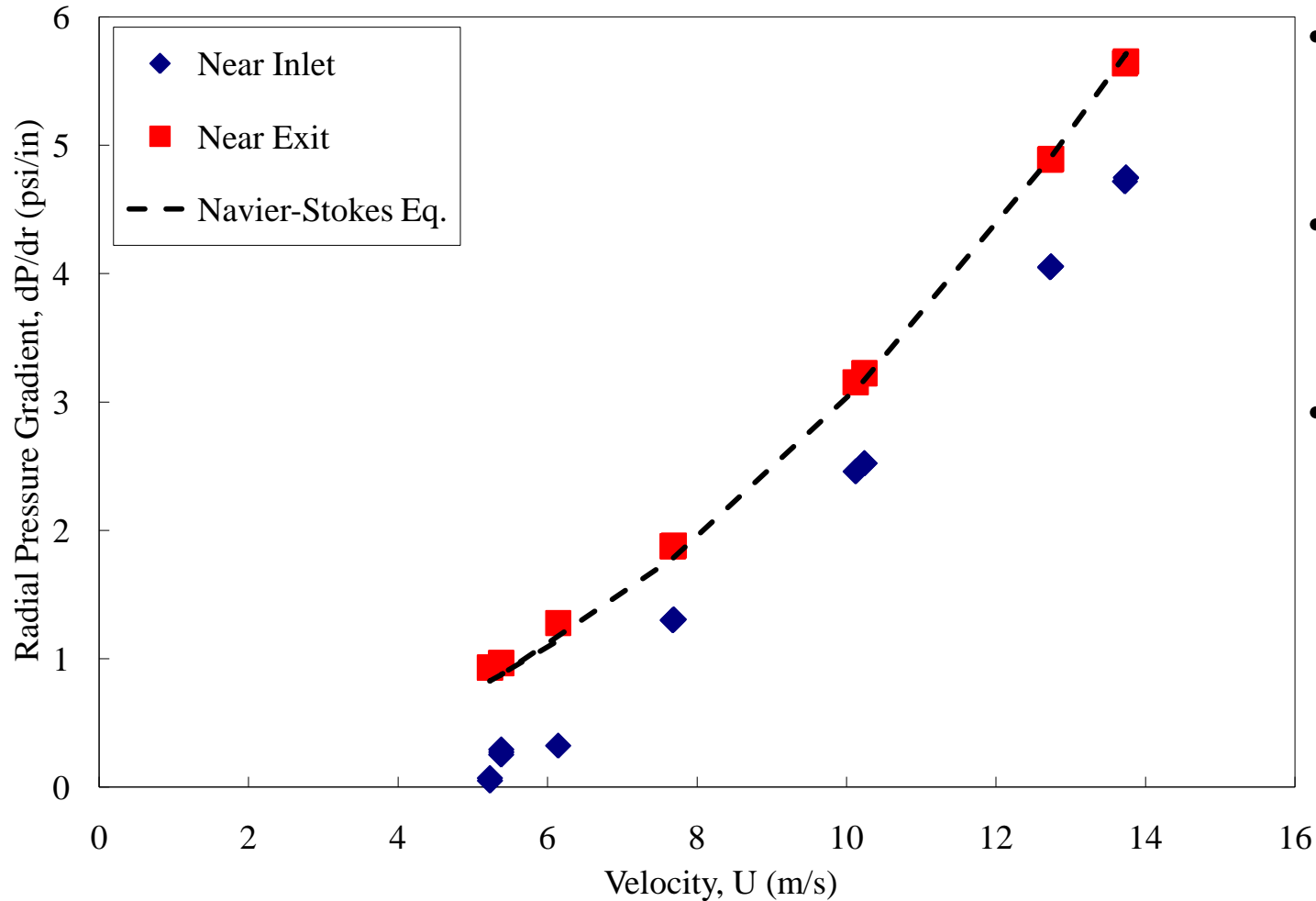
Conditions:

- $AR = 4$,
- $q'' = 130 \text{ W/cm}^2$,
- Exit location

- Slopes match
- All over predict data



Curvature Effects: Radial Pressure Gradients



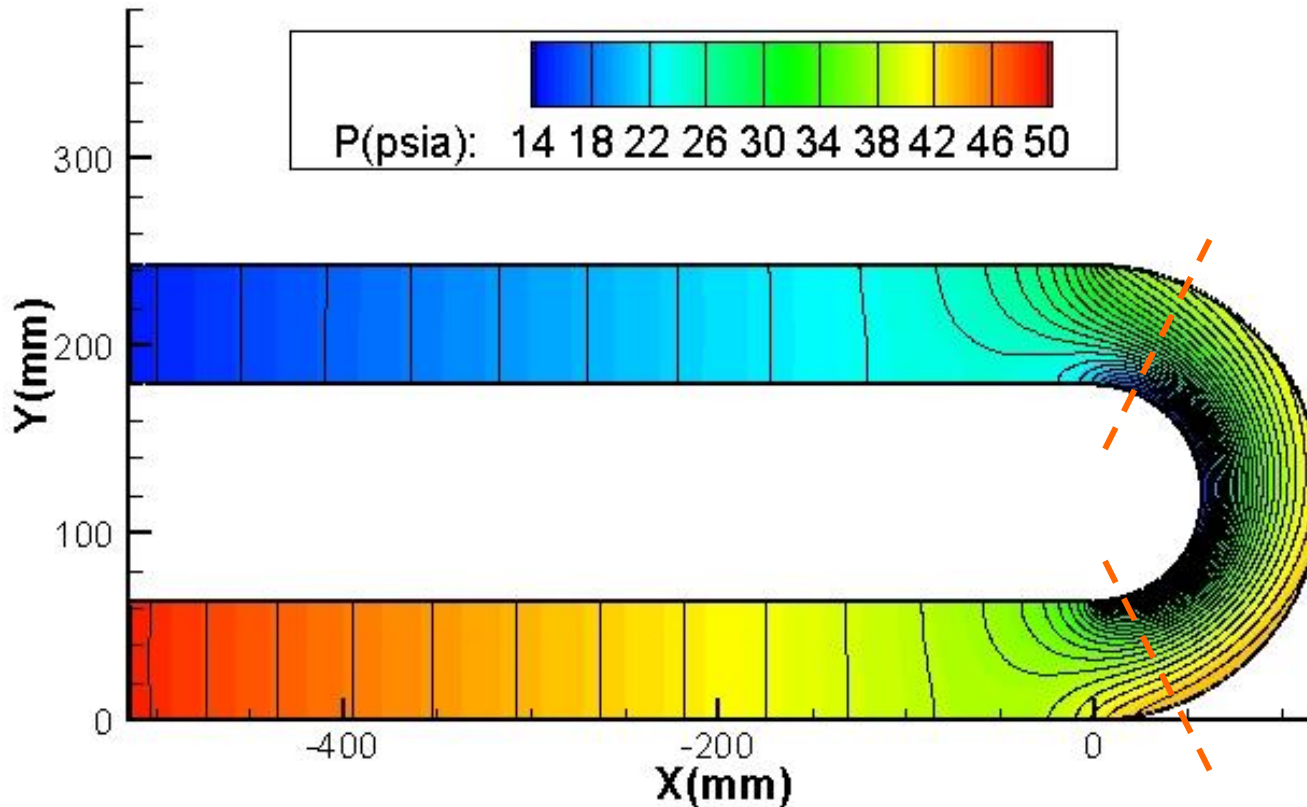
- fully developed flow in a circular curved channel
- No mean radial component of velocity
- Navier-Stokes equation for the radial direction becomes:

$$\frac{\rho v_{\theta}^2}{r} = \frac{dP}{dr}$$

DISTRIBUTION A, Approved for public release.



Curvature Effects: Radial Pressure Gradients (cont.)



Conditions:
 $AR = 10$
 $U = 15 \text{ m/s}$
 $T_{in} = 20 \text{ }^\circ\text{C case}$

- Radial pressure gradient begins forming $\sim 11 D_h$ upstream of inlet
- Persists $\sim 18 D_h$ downstream of the exit



Summary

- Correlation Analysis:
 - Correlations generated at each location captured data trend well
 - Correlations with viscosity ratio, and x/D terms capture over 96% of data within 10% of the prediction ($x/D_h \geq 15$)
 - Addition of published curvature terms captured data trend well at each location
 - Correlation able to predict heat transfer using design inputs, however limited to current test conditions
- Curvature Effects:
 - strength of radial pressure gradients directly relates to the centripetal acceleration
 - A reduced form of the Navier-Stokes equations predicted the near exit radial pressure gradient well
 - CFD radial pressure distributions showed the effects of curvature upstream and downstream of the curved channel
 - Radial pressure gradients begin forming $\sim 11 D_h$ upstream of the inlet
 - Persist ~ 18 hydraulic diameters downstream of the exit (AR 10, 15 m/s, 20°C)



Future Plans



- Curved Channel Testing
 - Complete AR = 1, 2, and 8
 - Revisit comparing to straight channel data – Curvature Enhancement
 - Assess friction factor
- Continue CFD effort
- Extend database to higher Re, higher q'' , different fluids (Phase II)

Questions ?



Data Reduction



- Convection Coefficient

$$q''(W + t_f) = \sum_i \bar{h}(T_i - T_b)\Delta s_i + q'_{fin,cond}$$

3 T/Cs
in neck

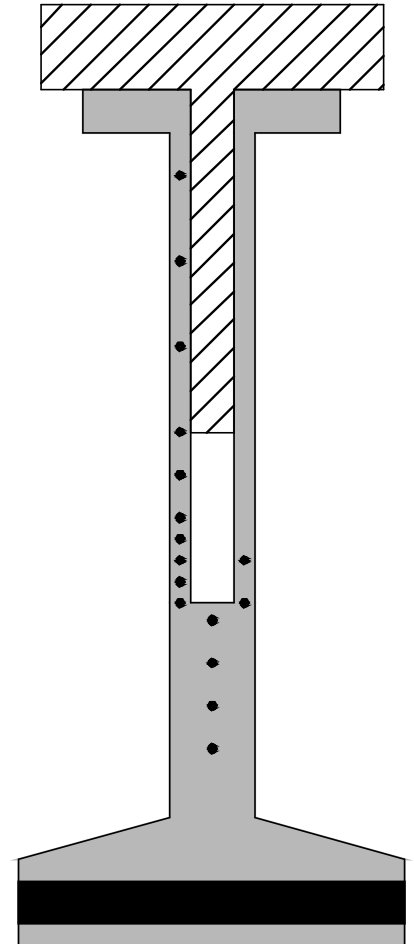
average \bar{h}
for cross-section
(3 walls)

bulk temp
assumption

fin temperature data

estimated from
fin temp gradient

$$Nu \equiv \frac{\bar{h}D_h}{k}$$





References



- Ito, H., 1959, “Friction Factors for Turbulent Flow in Pipes,” *ASME Journal of Basic Engineering*, Vol. 81, pp. 123-134.
- Sturgis, J.C. and Mudawar, I., “Single-Phase Heat Transfer Enhancement in a Curved, Rectangular Channel Subjected to Concave Heating,” *International Journal of Heat and Mass Transfer*, Vol. 42, pp. 1255-1272, 1999.
- Niino, M., Kumakawa, A., Yatsuyanagi, N. and Suzuki, A., ***Heat Transfer Characteristics of Liquid Hydrogen as a Coolant for the LO₂/LH₂ Rocket Thrust Chamber with the Channel Wall Construction***, Paper AIAA 82-1107, *18th AIAA/SAE/ASME Joint Propulsion Conference*, Cleveland, OH, 1982.
- Pratt, N.H., “The Heat Transfer in a Reaction Tank Cooled by Means of a Coil,” *Transactions of the Institution of Chemical Engineers*, Vol. 25, pp.163-180, 1947.